Solar Energy Materials & Solar Cells 247 (2022) 111937

Contents lists available at ScienceDirect

Solar Energy Materials and Solar Cells

journal homepage: www.elsevier.com/locate/solmat

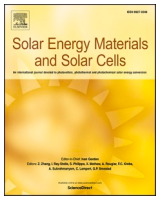

Thermal performance of nanofluids based on tungsten disulphide nanosheets as heat transfer fluids in parabolic trough solar collectors

Paloma Martínez-Merino [a], Patrice Estellé [b], Rodrigo Alcántara [a], Iván Carrillo-Berdugo [a], Javier Navas [a,*]

[a] Department of Physical Chemistry, University of Cádiz, E-11510, Puerto Real, Spain
[b] Univ of Rennes, LGCGM, EA3913, F-35000, Rennes, France

ARTICLE INFO

Keywords:
Nanofluids
Concentrating solar power
Heat transfers
Energy storage
Thermal properties

ABSTRACT

Nanofluids are considered as a new generation of heat transfer fluids since they exhibit thermophysical properties improvements compared with conventional heat transfer fluids. The high thermal conductivity of nanofluids and even the isobaric specific heat enhancements over conventional liquids make these colloidal suspensions very attractive in many research areas, including solar energy. In this work, nanofluids based on tungsten disulphide (WS_2) nanosheets have been prepared from the thermal oil currently used as heat transfer fluid in Concentrating Solar Power (CSP) plants. The high aspect ratio of WS_2 bidimensional nanostructures provides high long-term colloidal stability to the nanofluids and facilitates heat transport. Cetyltrimethylammonium bromide and polyethylene glycol have been used as surfactants to improve the exfoliation process and enhance the colloidal stability of the nanomaterial dispersions. Some properties such as density and viscosity of the base fluid have not been significantly altered by the presence of WS_2 nanosheets in the base fluid. However, studies on the thermal properties of nanofluids have shown promising results with increases in thermal conductivity of up to 33% and heat transfer coefficient by 21% over the base fluid. Furthermore, it has been estimated that the overall efficiency of the CSP system could be improved by 31% by replacing the conventional thermal fluid with 2D-WS_2-based nanofluids.

1. Introduction

The term nanofluid was introduced for the first time in 1995 by Choi in the Argonne National Laboratory [1]. These colloidal suspensions of nano-sized particles in a liquid medium have been of interest to scientists since its discovery. In contrast to conventional heat transfer fluids, nanofluids exhibit high thermal conductivities and heat transfer coefficients [2–6]. The addition of solid nanoparticles to a fluid can lead to a suspension with improved thermophysical properties as solids exhibit higher thermal conductivity values than liquids. In addition, the high specific surface area of nanoparticles prevents the settling problems inherent in fluids with micrometric or millimetric particles [7,8]. As a result of their interesting properties, nanofluids are being studied in a plethora of engineering applications such as electronic applications [9,10], solar energy systems [11–13], cooling systems [14–16] or biomedical applications [17–19]. In recent years, attention has been focused on the use of nanofluids as heat transfer fluids in concentrating solar power (CSP) plants [20,21]. Concentrating solar power is considered as a clean, renewable and sustainable energy with a significant energy potential to become an alternative to polluting fossil fuel-based technologies. The operational principle of CSP systems lies in the use of mirrors that reflect incident solar radiation onto a receiver where solar energy is converted into useful heat. Among CSP collectors, parabolic trough collectors (PTC) are the most mature technology, comprising almost 90% of the currently CSP technology installed worldwide [22,23]. In CSP plants based on parabolic trough collectors, concave mirrors reflect incoming sunlight onto an absorber tube located at the focal line of the collectors. The absorber tube, coated with a selective absorber material, contains a heat transfer fluid (HTF) which reaches high temperatures. The thermal energy absorbed by the HTF is transferred to the power block to produce electricity through a thermodynamic Rankine cycle [24–26]. However, one of the factors hindering the growth of CSP energy is its high levelized cost. Considerable efforts are being made to reduce the capital cost of CSP and make it comparable to other electricity generation options [27–29]. In this regard, the replacement of the thermal oil used in the absorber tubes of PTC collectors with nanofluids has been explored over the last few years

* Corresponding author.
E-mail address: javier.navas@uca.es (J. Navas).

https://doi.org/10.1016/j.solmat.2022.111937
Received 4 May 2022; Received in revised form 23 June 2022; Accepted 29 July 2022
Available online 29 August 2022

Nomenclature

Cp	[J kg^{-1} K^{-1}] Isobaric specific heat
D	[m^2 s^{-1}] Thermal diffusivity
Di	[m] Inner pipe diameter
h	[Wm^{-2} K^{-1}] Heat transfer coefficient
Vav	[m^3s^{-1}] Average fluid velocity in the inner pipe
Nu	[−] Nusselt number
Pr	[−] Prandtl number
Re	[−] Reynolds number
φ	[−] Efficiency
Φ	[%] Volume fraction
k	[W m^{-1} K^{-1}] Thermal conductivity
λ	[m] Wavelength
μ	[Pa s] Dynamic viscosity
ρ	[kg m^{-3}] Density

Subscripts

bf	Base fluids
coll	Collector
exch	Exchanger
nf	nanofluid
nm	Nanomaterial
sys	System

Abbreviations

CSP	Concentrated Solar Power
CTAB	Cetyltrimethylammonium bromide
DLS	Dynamic Light Scattering
HTF	Heat Transfer Fluid
LFA	Laser Flash Analysis
LPE	Liquid Phase Exfoliation
PEG	Polyethylene glycol
PTC	Parabolic Trough Collector
TEM	Transmission Electron Microscopy
TMDSC	Temperature Modulated Differential Scanning Calorimetry
UV–Vis	Ultraviolet–Visible

with the aim of increasing the thermal efficiency of CSP plants [30,31]. Currently, the most commonly used heat transfer fluid in CSP collectors is an eutectic mixture of biphenyl and diphenyl oxide that is capable of reaching temperatures of up to 400 °C without decomposing [32]. In the literature, the vast majority of nanofluid studies use water [33] as the base fluid or molten salts for high temperature applications [34,35] instead of this kind of thermal oil [36] or silicone oils which are being studied in recent times [37,38]. In addition, it is necessary to open up the research area to other nanoparticles besides the typical metals and metal oxide already studied [39–41].

Therefore, the study of nanofluids based on the eutectic mixture of biphenyl and diphenyl oxide as the base fluid should be developed in order to optimize this kind of nanofluid for being applied in CSP plants due to the need to improve the overall efficiency of this kind of plants. Also, to analyse the effect of the use of nanofluids in CSP plants should be performed for knowing the performance of nanofluidos for this application. Some previous work have been performed about this topic using several nanomaterials, typically metals such as Pd nanoplates [42] or metal oxides as CuO [43]. But, advanced nanomaterials with amazing properties should be tested in order to maximise the performance of nanofluidos in this application. Thus, the present work addresses the research of nanofluids based on two-dimensional tungsten disulphide nanostructures as heat transfer fluid in CSP plants. The 2D morphology of the nanomaterial provides advantageous characteristics to the nanofluids in comparison to classical spherical nanoparticles. Hence, the higher aspect ratio of nanosheets increases the colloidal stability of the resulting nanofluids. Furthermore, heat is transferred faster through nanosheet networks than through isolated spherical nanoparticles dispersed in the fluid. Tungsten disulphide is a layered compound where a hexagonally packed of W atoms are sandwiched between two layers of S atoms. Within the layers, the atoms are bound by covalent bonds, but the layers are held to each other by weak Van Der Waals interactions [44–46]. As a consequence of these weak interactions, bulk WS_2 can be easily exfoliated and separated into nanolayers. In this work, nanofluids based on WS_2 nanosheets have been prepared through the liquid phase exfoliation procedure. Cetyltrimethylammonium bromide and polyethylene glycol have been used to obtain a high efficiency in the exfoliation process. The resulting nanofluids have been studied from the point of view of their stability and thermal properties. Finally, in order to assess the feasibility of the prepared nanofluids, the increase in efficiency of different CSP configurations with the implementation of 2D-WS_2-based nanofluids has been analytically estimated.

2. Materials and methods

2.1. Preparation of 2D-WS_2-based nanofluids

Nanofluids based on WS_2 nanosheets were prepared by the liquid phase exfoliation (LPE) technique. In this technique, WS_2 films are separated from the bulk material by applying ultrasound in a given solvent [47,48]. However, not all solvents are suitable for the exfoliation of WS_2. The necessary condition is that the polar and dispersive components of the surface tension of the solid should be similar to those of the solvent [49]. In previous works, the modification of the ratio of the surface tension components of the Dowtherm A™ fluid by the addition of different surfactants has been studied [50,51]. Dowtherm A™ is a eutectic mixture of biphenyl ($C_{12}H_{10}$, 16.5%) and diphenyl oxide ($C_{12}H_{10}O$, 73.5%) and is currently the most widely used heat transfer fluid in the absorber tubes of parabolic trough collectors in concentrating solar power plants. In this work, polyethylene glycol (PEG, average molecular mass ≈ 200) and cetyltrimethylammonium bromide (CTAB) were used as surfactants to reduce the ratio between the polar and dispersive components of the surface tension of Dowtherm A™ until it approached the characteristic ratio of the surface tension components of WS_2. Therefore, six nanofluids were prepared with different concentrations of CTAB and PEG-200.

Briefly, 15 mg of WS_2 (nanopowder 90 nm, purity ≈ 99%) and 5 ml of a surfactant (CTAB or PEG-200) solution in Dowtherm A™ were added to four vials. The mixture of base fluid and WS_2 was dispersed in an Elmasonic P30H ultrasonic bath at a frequency of 80 kHz for several hours. Table 1 specifies the surfactant concentrations and sonication time used for each nanofluid. Subsequently, the dispersions were centrifuged first 10 min at 1000 rpm and then the supernatant was centrifuged for 10 min at 4000 rpm to remove any remaining non-exfoliated material and agglomerates. The supernatant obtained after the second centrifugation would constitute the resulting nanofluid.

Table 1
Details and identification of the 2D-WS_2-based nanofluids.

Nanofluid label	wt.% surfactant	Sonication time/h
Nf 1	$9{\cdot}10^{-3}$ wt% CTAB	4
Nf 2	$9{\cdot}10^{-3}$ wt% CTAB	8
Nf 3	$1.1{\cdot}10^{-2}$ wt% CTAB	8
Nf 4	0.2 wt% PEG-200	8
Nf 5	0.2 wt% PEG-200	4
Nf 6	0.75 wt% PEG-200	4

2.2. Characterisation of 2D-WS_2-based nanofluids

Transmission electron microscopy (TEM) was performed on a JEM-2100 F microscope to determine the size of the WS_2 nanomaterial and to check the two-dimensional morphology obtained by the LPE method. The stability of the nanofluids was measured for 15 days using several techniques due to the fundamental role that stability plays in the proper performance of the nanofluids [52,53]. Firstly, the sedimentation of the nanomaterial in the nanofluids was evaluated by UV–Vis spectroscopy monitoring. A USB2000+ spectrometer and a DH-2000-BAL halogen lamp supplied by Ocean Optics® were used. Spectra were recorded between 300 and 900 nm and the change of the extinction coefficient at a fixed wavelength of $\lambda = 629$ nm was evaluated over time. Dynamic light scattering is the other technique for assessing the temporal colloidal stability of nanofluids. By this technique, the size of the agglomerates in nanofluids is determined. The study of this parameter over time provides information on the formation of agglomerates of considerable size that could sediment. Particle size measurements were carried out with a Zetasizer Nano ZS equipment supplied by Malvern Instruments Ltd®. In addition, other properties that influence the heat transfer of the nanofluids such as density and viscosity were determined. The density was estimated by pycnometry and the dynamic viscosity by means of a Kinexus Pro stress-controlled rheometer supplied by Malvern Instruments Ltd®. Those properties were evaluated following the procedures previously described in Ref. [46]. Regarding the thermal properties, the isobaric specific heat was analysed using the technique of temperature-modulated differential scanning calorimetry in a DSC 214 Polyma calorimeter supplied by Netszch®. The methodology established to determine the isobaric specific heat of the nanofluids in a temperature range between 20 and 90 °C has been reported in previous studies [54]. The thermal conductivity was deduced from the thermal diffusivity data obtained using the LFA 1600 equipment supplied by Linseis®. According to the ASTM E1461-01 standard, thermal conductivity (k) can be calculated as a function of thermal diffusivity (D), density (ρ) and isobaric specific heat (C_P) by the formula $k(T) = D(T)\cdot C_P(T)\cdot\rho(T)$. The thermal conductivity values were determined at temperatures between 20 and 90 °C.

3. Results and discussion

Fig. 1 shows the nanostructures found in the prepared nanofluids. Partial exfoliation was evident in the sample extracted from nanofluid Nf 1 (Fig. 1a) as even though some nanosheets are split from the 3D material there are still dark areas associated with bulk material that has not been exfoliated. In Nf 2, the nanostructures obtained (Fig. 1b) showed a higher electron transparency but also agglomerates of sizes of up to 500 nm were detected. In contrast, in Nf 3, highly electron transparent and well-defined nanosheets with lateral sizes at 100–120 nm were observed. Therefore, in the case of nanofluids prepared with CTAB, increasing the ultrasonication time and surfactant concentration favoured the exfoliation process. In nanofluids containing PEG-200, stacked and non-exfoliated material were found in samples prepared with the lowest concentration of PEG-200, i.e. with 0.2 wt% PEG-200 (Fig. 1d and e). Conversely, the characteristic nanostructures in Nf 6 were isolated and well-defined WS2 nanosheets of 50 nm lateral sizes. Hence, increasing the surfactant concentration was a more decisive factor than the ultrasonication time to achieve an efficient exfoliation in the nanofluids prepared with PEG-200 solutions. Accordingly, TEM images have proved the efficiency of the LPE process to obtain nanofluids based on WS2 nanosheets being the nanofluids Nf 3 and Nf 6 the ones containing better defined and less agglomerated nanosheets (see Fig. 2).

Temporal colloidal stability analysis by UV–Vis spectroscopy revealed that nanofluids prepared with PEG-200 surfactant had a higher extinction coefficient than nanofluids prepared with CTAB. This result means that in the nanofluids prepared with PEG the concentration of WS_2 nanosheets is higher and consequently they could exhibit improved thermal properties compared to the nanofluids prepared with CTAB. Fig. 3 shows the evolution of the extinction coefficient of WS_2 based nanofluids at a wavelength of 629 nm, where there is a characteristic band of WS_2 [55]. The nanofluid Nf 1 was no longer measured after the ninth day as the extinction coefficient values were close to zero. The initial value of the extinction coefficient in this nanofluid is low, suggesting that exfoliation has not been successful in this case. This result is consistent with the microscopy study which revealed areas of unexfoliated WS_2 material and the formation of large agglomerates of nanomaterial in nanofluid Nf 1. Constant extinction coefficient values over

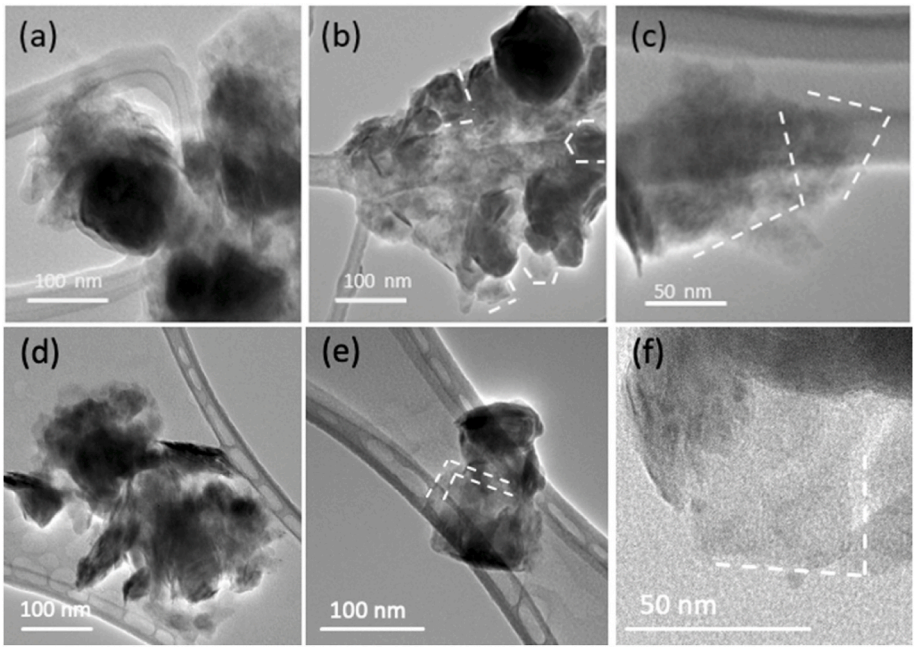

Fig. 1. WS_2 nanostructures obtained by the LPE method. Figures a, b and c correspond to the nanostructures found in the nanofluids prepared with CTAB (Nf 1, Nf 2 and Nf 3 respectively) and figures d, e and f refer to the nanostructures found in the nanofluids prepared with PEG (Nf 4, Nf 5 and Nf 6 respectively).

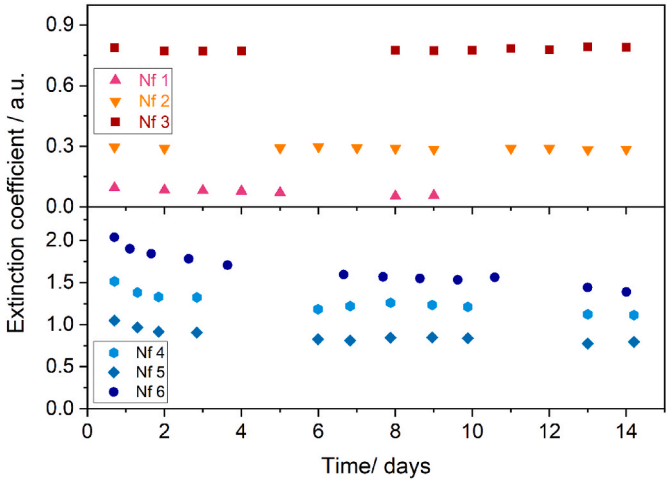

Fig. 2. Time evolution of the extinction coefficient at λ = 629 nm for nanofluids based on WS_2 nanosheets. In the upper part, the results of the nanofluids prepared with CTAB (Nf 1, Nf 2, and Nf 3) are shown. The bottom graph shows the values for the nanofluids in which PEG was used as surfactant (Nf 4, Nf 5 and Nf 6).

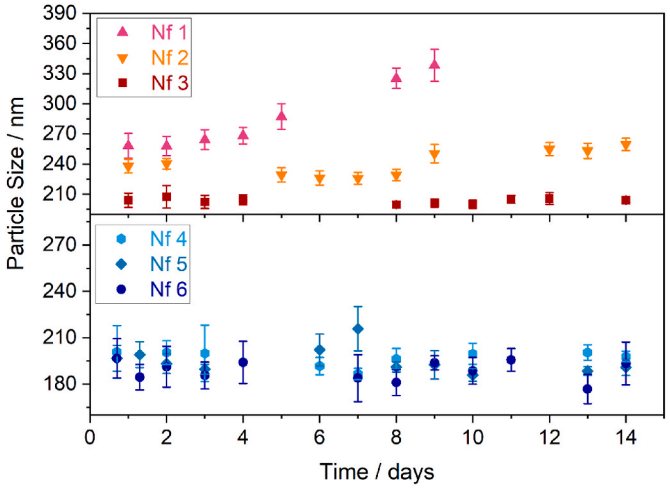

Fig. 3. Temporal evolution of the particle size of the agglomerates contained in the 2D-WS_2-based nanofluids. The top graph shows the evolution of the particle size in the nanofluids prepared with CTAB (Nf 1, Nf 2 and Nf 3) and the bottom graph shows those of the nanofluids prepared with PEG (Nf 4, Nf 5 and Nf 6).

time were observed in the nanofluids Nf 2 and Nf 3, evidencing the high colloidal stability of these systems. In the case of nanofluids prepared with PEG, a slight decrease of the extinction coefficient in the first days of characterisation took place which is attributed to the sedimentation processes. However, from the sixth day onwards, these nanofluids show stable extinction coefficient values, which verifies their high long-term stability.

The temporal study of the particle size evolution obtained by DLS (Fig. 3) showed that in nanofluid Nf 1, the particle size increased rapidly, which is associated with the agglomeration of WS_2 nanostructures. Because of the low extinction coefficient values and the increase in particle size, nanofluid Nf 1 was no longer characterised after the ninth day. In the nanofluid Nf 2, a moderate increase in the size of agglomerates is observed, reaching a value of 260 nm. Nf 3 is the nanofluid with the smallest and constant particle size compared to the rest of the CTAB systems. The nanofluids prepared with PEG showed constant particle size values over time of around 180–210 nm. Of the systems composed of CTAB and PEG, the nanofluids Nf 3 and Nf 6 are the most promising in their category to be evaluated. According to TEM analysis and colloidal temporal stability studies, in these nanofluids the concentration of defined and stable nanosheets is higher than in the rest of the prepared WS_2 nanofluids. Therefore, the characterisation of rheological and thermal properties will focus on the nanofluids Nf 3 and Nf 6.

Density is one of the properties of nanofluids that is relevant in heat transfer processes. An increase in density is commonly associated with an increase in the amount of nanomaterial involved in enhancing the thermal conductivity of the system [56,57]. Table 2 shows the density of nanofluids and Dowtherm A™ measured at 25 °C by pycnometry. Henceforth, the Dowtherm A™ fluid will be referred as HTF (Heat Transfer Fluid). The density of HTF is increased up to 0.59% with the presence of WS_2 nanosheets and surfactant. From the density data, the volume fraction of nanomaterial in Nf 3 and Nf 6 nanofluids has been calculated. The volume fraction is expressed as $\Phi = 100\cdot((\rho_{nf} - n_{bf})/(\rho_{nm} - n_{bf}))$ where the subscripts nf, bf and nm refer to nanofluid, base fluid and nanomaterial. The density of WS_2 is 7500 kg m^{-3} [58]. The nanofluid Nf 6 has the highest volume fraction which is also the nanofluid with the highest extinction coefficient.

Fig. 4 represents the dynamic viscosity values of HTF and nanofluids Nf 3 and Nf 6 with increasing temperature. Here, only dynamic viscosity values are reported because of the Newtonian behaviour experimentally observed. Viscosity is a property of fluids that can affect flow rate, pumping power, pressure drop and convective heat transfer [59,60]. High increases in the viscosity of the base fluid when introducing nanomaterial is detrimental to its application in pipelines. The experimentally measured viscosity of HTF is 3.89 mPa s which differs just 0.4% from the value reported by the supplier. The viscosity of the nanofluids follows the same decreasing trend with temperature as HTF. The maximum increase in viscosity with respect to HTF is obtained for the nanofluid Nf 6, which is only 1.7%. The nanofluid Nf 6 is the one with the highest volumetric concentration of WS_2 nanosheets, which explains this increase in viscosity. However, the increase in viscosity is low (as is observed in Fig. 4), and lower than experimental uncertainty, which indicates that the use of these nanofluids would not increase the pumping power required in solar power plants and would not compromise the heat transfer.

The thermal properties of the samples as a function of temperature were plotted in Fig. 5. The isobaric specific heat values of the nanofluids (Fig. 5a) follow the same increasing trend with temperature as those of the base fluid. In the nanofluid Nf 3 (prepared with $1.1\cdot10^{-2}$ wt% CTAB), the isobaric specific heat is 1.5% lower than that of the HTF. Several experimental works have reported a decrease of the isobaric specific heat in nanofluids compared to the base fluid [61,62]. The lower isobaric specific heat of solids compared to liquids justifies these results. However, the opposite trend has been reported in nanofluid Nf 6 (prepared with 0.75 wt% PEG-200), i.e. an increase of the isobaric specific heat by up to 6.5% compared to HTF. It is noteworthy that despite the characteristics of the solid and the base fluid, the properties of nanofluids are not a simple combination of the properties of their separate components. Therefore, interactions between the nanomaterial and the fluid and surfactant molecules also contribute to the unexpected increase in isobaric specific heat. Previous works have reported increases in isobaric specific heat of nanofluids in relation to base fluids [63–65]. Based on the fact that nanostructures induce restructuring of the liquid close to their interface, a plausible explanation for the anomalous increase of the isobaric specific heat is the formation of an ordered

Table 2
Density, density increment and volume fraction of samples.

Sample	Density/kg·m^{-3}	Density increase/%	Φ/vol%
HTF	1056.6 ± 0.5	–	–
Nf 3	1060.8 ± 1.4	0.40	0.065
Nf 6	1062.8 ± 0.2	0.59	0.096

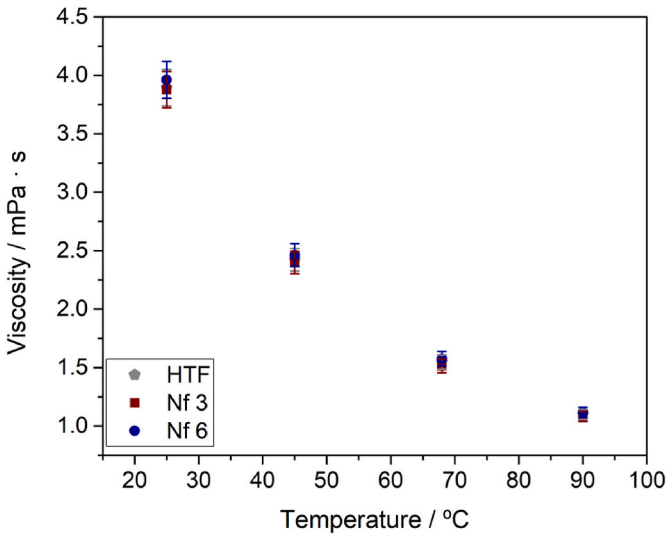

Fig. 4. Dynamic viscosity values of WS_2 nanofluids and base fluid with respect to temperature.

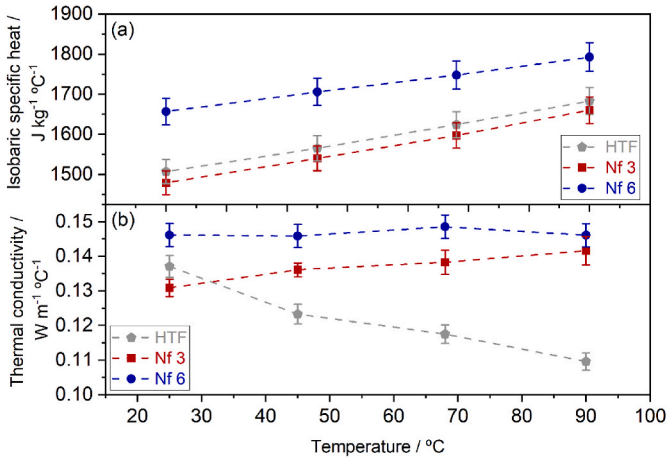

Fig. 5. Values of isobaric specific heat (a) and thermal conductivity (b) of samples Nf 3, Nf 6 and HTF with increasing temperature.

semi-solid layer of liquid on the surface of the nanomaterial [66,67]. The thermal resistance at the interface will be different depending on the arrangement of the liquid and surfactant molecules around the nanostructure, which depends on the nature of the surfactant and the liquid. Thus, it is observed that the isobaric specific heat of the HTF can be increased or decreased by the addition of WS_2 nanosheets depending on the presence of CTAB or PEG-200 molecules in the medium.

Fig. 5b shows the thermal conductivity values of the nanofluids and the base fluid in a temperature range from 25 to 90 °C. The thermal conductivity of the HTF follows a decreasing trend with temperature while in the nanofluids the thermal conductivity increases slightly with temperature. The thermal conductivity of nanofluids Nf 3 (prepared with $1.1{\cdot}10^{-2}$ wt% CTAB) and Nf 6 (prepared with 0.75 wt% PEG-200) are 29% and 33% higher than that of HTF at 90 °C. These results are consistent with those previously discussed in the extinction coefficient and volume fraction analyses. The nanofluid prepared in a PEG-200/HTF system has the highest thermal conductivity values and also presents the highest extinction coefficient and volume fraction values. Therefore, the exfoliation process is more effective with PEG than with CTAB and more amount of WS_2 nanosheets are obtained which results in a higher increment of the thermal conductivity. The different behaviour of the thermal conductivity of the samples evidences different heat transfer mechanisms in the 2D-WS_2-based nanofluids with respect to the base fluid. In the literature, there is no consensus on the dominant mechanism responsible for the enhancement of heat conduction in nanofluids. Some of the most widely accepted theories of thermal conductivity mechanisms in nanofluids are founded on the Brownian motion of the particles [68], liquid layering at the liquid/particle interface [69], thermophoresis [70] or the effect of nanoparticle clustering [71]. In addition, several authors have highlighted the relevance of the shape of the nanostructures on the effective thermal conductivity of the suspension [72–75]. These possible mechanisms are specific for nanofluids and they can explain the reason of the different behaviour of the nanofluidos and the base with respect to temperature. Hence, in the case of two-dimensional nanostructures such as the WS_2 nanosheets studied in this work, the high aspect ratio leads to a network chain structure, providing paths for rapid heat transport along the in-plane direction. However, it is difficult to state the main mechanism responsible for the heat conduction in the prepared nanofluids. Probably, the increase in thermal conductivity will be governed by several factors such as the bidimensional structure, the thermal resistance at the interface of the solid or the clustering phenomenon.

To determine the thermal performance of the nanofluids, the heat transfer coefficient, h [70,76], has been determined. This coefficient can be calculated from the following formula:

$$h = \frac{Nu \cdot k}{D_i} \tag{1}$$

where Nu represents the Nusselt number, k is the thermal conductivity value and D_i is the internal diameter of the pipe through which the nanofluid flows (considered here as 0.066 m [69]). The Nusselt number is obtained from the following mathematical expression:

$$Nu = 0.023 Re^{0.8} \cdot Pr^{0.4} \tag{2}$$

where Re represents the Reynolds number and Pr is referred to the Prandtl number. These parameters are defined by the equations:

$$Re = \frac{\rho \cdot V_{av} \cdot D_i}{\mu} \tag{3}$$

$$Pr = \frac{\mu \cdot C_P}{k} \tag{4}$$

In the above equations ρ, μ, C_P and k are respectively the density, viscosity, isobaric specific heat and thermal conductivity of the fluid. The term V_{av} refers to the mean flow rate and is calculated as $V_{av} = 4{\cdot}V/(\pi \cdot R_i^2)$ where R_i is the internal radius of the pipe. Fig. 6 shows the heat transfer coefficient values of the base fluid and the nanofluids at flow rates of 100 L min^{-1}, 200 L min^{-1} and 300 L min^{-1}. The heat transfer coefficient of the samples increases with increasing flow rate and temperature, which is beneficial considering that solar plants operate at high temperatures, up to 400 °C. Based on these results, the heat transfer is expected to be even more effective under real application conditions. The heat transfer coefficient of nanofluids is higher in all cases than that of HTF. At 90 °C, the improvement is 17.1% for nanofluid Nf 3 (prepared with $1.1{\cdot}10^{-2}$ wt% CTAB) and 21.5% for nanofluid Nf 6 (prepared with 0.75 wt% PEG) when compared to the heat transfer coefficient of HTF. Therefore, the nanofluids based on WS_2 nanosheets prepared in this work constitute a significant breakthrough over the heat transfer fluid currently used in solar power plants. In order to assess the implications of the use of these nanofluids in solar plants, a theoretical study is performed on the increase in collector efficiency, heat exchanger efficiency and overall CSP system efficiency when 2D-WS_2-based-nanofluids are incorporated.

The efficiency of the CSP system has been estimated when the typical heat transfer fluid is replaced by nanofluids Nf 3 (prepared with $1.1{\cdot}10^{-2}$ wt% CTAB) and Nf 6 (prepared with 0.75 wt% PEG-200). The overall efficiency of the system is influenced by the efficiency of the

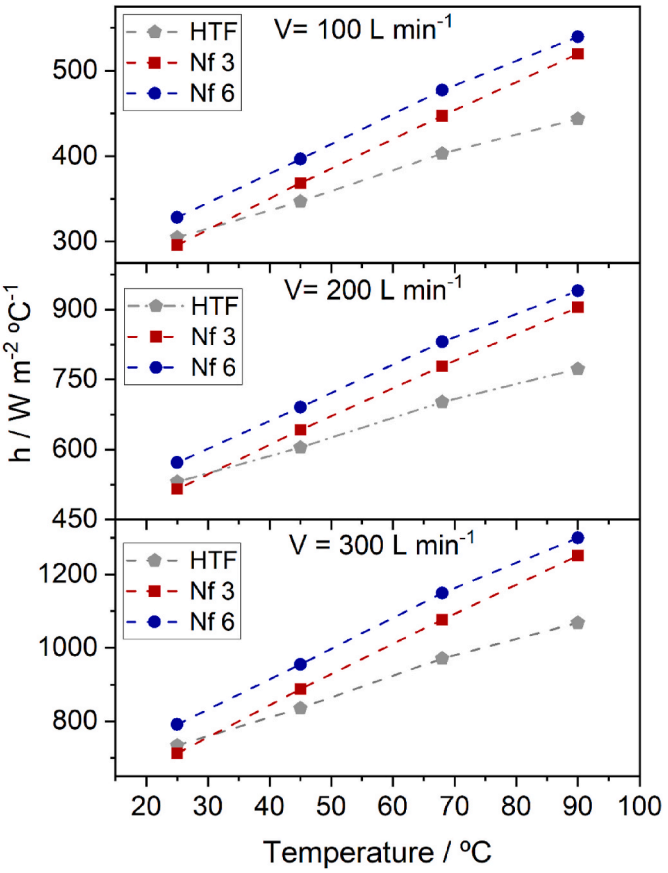

Fig. 6. Heat transfer coefficient of 2D-WS_2-based nanofluids and HTF at different flow rates.

collector and of the heat exchanger. In the case of collector efficiency, an analytical approach has been performed considering a surface collector configuration and also a volumetric collector configuration. On the basis of the expressions of Bellos [77] and O'Keeffe [78], the length of the absorber tube to reach a temperature of 300 °C for both types of collectors was determined. This is the maximum working temperature at which the Dowtherm A™ thermal oil can be used without degradation risk and therefore it would be the temperature at which the maximum efficiency is achieved. The available experimental data are limited to temperatures below the operating due to the limitations of the measurements' techniques. Input data for these models at higher temperature is therefore estimated by using fitting functions for extrapolation Fig. 7 shows the length of the collector tube as a function of the outlet temperature for each of the configurations under study. The outlet temperature reaches a value of 300 °C when using a tube length of 249 m in the typical surface collector configuration using HTF. The estimated tube length for the same configuration using Nf 3 and Nf 6 nanofluids is very similar, being 250 and 252 m respectively. A volumetric manifold using HTF is not suitable because of the clear colouration of this fluid. Volumetric PTC collectors require the fluid a highly coloured fluid since the fluid itself serves as an absorbent, eliminating the selective coatings characteristic of other types of collectors. The tube lengths to reach the maximum outlet temperature using nanofluids Nf 3 and Nf 6 in a volumetric PTC are 263 and 265 m respectively. The expressions used to calculate the collector tube length, the outlet temperature and the efficiency of the CSP system components are detailed in the Supplementary Material. The thermal efficiency of the collector, ψ_{coll}, is determined from the research of Bellos et al. [77] and O'Keeffe et al. [78], while the heat exchanger effectiveness, ψ_{exch}, was estimated by using the NTU (number of transfer units) method [79]. The overall efficiency of the CSP system is finally calculated by $\psi_{sys} = \psi_{coll} \cdot \psi_{exch}$. As is shown in Fig. 8,

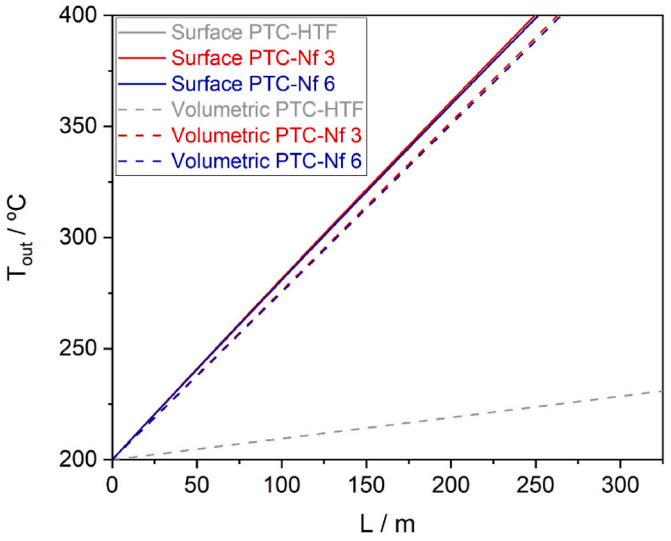

Fig. 7. Outlet temperature in surface and volumetric collectors depending on the length of the collector tube using the typical eutectic mixture of biphenyl and diphenyl oxide (HTF) and when the nanofluids Nf 3 and Nf 6 are used.

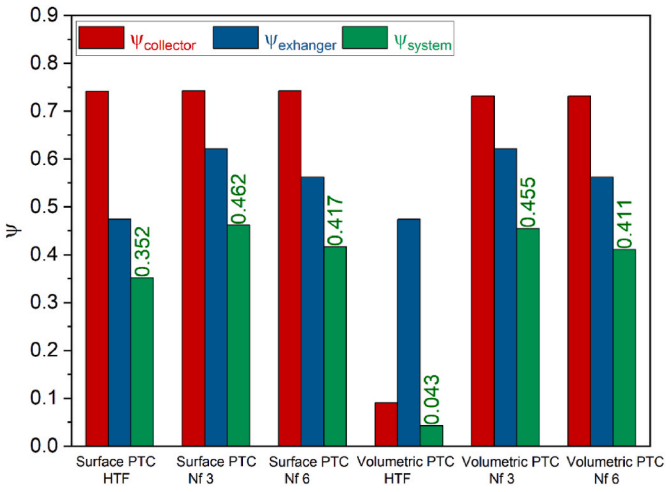

Fig. 8. Efficiency of the collector, heat exchanger and CSP system for the surface and volumetric collector configurations using the different samples under study.

the highest efficiency of the system is achieved with a configuration based on a surface PTC collector using Nf 3. The incorporation of this nanofluid provides a substantial efficiency increase of 31% over a surface PTC using Dowtherm A™. Nanofluid Nf 6 also achieves 18% higher performance in a PTC surface collector than in the equivalent HTF system. In a configuration based on a volumetric collector, improvements of 29% and 16% are also obtained compared to the system currently used (surface PTC using HTF) when nanofluids Nf 3 or Nf 6 are implemented. Although the collector tube length is longer to reach the outlet temperature and the performance is slightly lower than that of a surface collector, volumetric collectors using nanofluids are an attractive option as the selective coating costs required in a surface PTCs are eliminated. Therefore, it has been concluded that the 2D-WS_2-based nanofluids prepared in this work can be considered as a potential alternative to the use of conventional HTFs because of the high efficiency improvements that could be achieved with their application in CSP plants. Furthermore, the use of these nanofluids allows the implementation of cost-saving volumetric collectors.

4. Conclusions

Nanofluids based on 2D-WS_2 nanostructures have been prepared from a thermal oil typically used as heat transfer fluid in CSP systems. CTAB and PEG-200 were used as surfactant to increase the effectiveness of the LPE process and to improve the stability of the nanofluid. The colloidal stability results revealed that an increase in ultrasound time and surfactant concentration improves the stability of the nanofluids prepared with CTAB. In the case of nanofluids prepared with PEG-200, the increase of surfactant concentration was the most decisive factor to achieve a high concentration of stable nanomaterial dispersed in the base fluid. The agglomerate size in the stable nanofluids prepared with CTAB was around 200–250 nm while in the nanofluids prepared with PEG-200, the agglomerate size was about 180 nm. The viscosity of the base fluid only increases to a maximum of 1.5% in the presence of WS_2 nanosheets and surfactant. This slight increase is manageable and would not lead to pressure drops problems in the pipes of CSP plants. The most remarkable results were found in the analysis of the thermal properties. The nanofluids Nf 6 (prepared with 0.75 wt% PEG-200 and 4 h of sonication) and Nf 3 (prepared with 0.011 wt% CTAB and 8 h of sonication) exhibited an increase in thermal conductivity of 33% and 29% respectively compared to the base fluid. Also, the Nf 6 nanofluid showed an isobaric specific heat value 6.5% higher than that of the HTF. Improvements in thermal conductivity and isobaric specific heat led to an increase in the heat transfer coefficient by 21% in the nanofluid Nf 6 and 17% in the nanofluid Nf 3 compared to the base fluid. In addition, numerical efficiency analyses have demonstrated that the efficiency of the CSP system increases by 31% or 18% if Nf 3 nanofluid or Nf 6 nanofluid were used instead of the currently used thermal oil. Although the estimated efficiency for a volumetric collector using 2D-WS_2-based nanofluids is slightly lower than that of a surface collector using nanofluids, this efficiency is higher than that obtained with the surface collector configuration using the thermal oil commonly used at the present time. Therefore, the 2D-WS_2- based nanofluids prepared in this work are a potential alternative to the thermal oil used in solar plants and would also allow the adoption of volumetric collectors which are more cost-effective than conventional surface PTC collectors.

CRediT authorship contribution statement

Paloma Martínez-Merino: Writing – original draft, Methodology, Investigation. **Patrice Estellé:** Writing – review & editing, Investigation. **Rodrigo Alcántara:** Writing – review & editing, Supervision. **Iván Carrillo-Berdugo:** Formal analysis. **Javier Navas:** Writing – review & editing, Supervision, Project administration, Funding acquisition.

Declaration of competing interest

The authors declare that they have no known competing financial interests or personal relationships that could have appeared to influence the work reported in this paper.

Data availability

The authors do not have permission to share data.

Acknowledgements

We acknowledge Ministerio de Ciencia e Innovación y del Gobierno de España for financial support related to measurements of thermal properties, which were carried out using devices acquired under Grant No. UNCA15-CE-2945. Also, this work has been co-financed by the 2014–2020 ERDF Operational Programme and by the Department of Economy, Knowledge, Business and University of the Regional Government of Andalusia. Project reference: FEDER-UCA18-107510.

Appendix A. Supplementary data

Supplementary data to this article can be found online at https://doi.org/10.1016/j.solmat.2022.111937.

References

[1] S.U.S. Choi, J.A. Eastman, Enhancing thermal conductivity of fluids with nanoparticles, in: ASME International Mechanical Engineering Congress and Exhibition, San Francisco, CA (United States), 1995.
[2] R. Lenin, P.A. Joy, C. Bera, A review of the recent progress on thermal conductivity of nanofluid, J. Mol. Liq. 338 (2021).
[3] L. Godson, B. Raja, D.M. Lal, S. Wongwises, Enhancement of heat transfer using nanofluids-An overview, Renew. Sustain. Energy Rev. 14 (2010) 629–641.
[4] C. Kleinstreuer, Y. Feng, Experimental and theoretical studies of nanofluid thermal conductivity enhancement: a review, Nanoscale Res. Lett. 6 (2011).
[5] M. Raja, R. Vijayan, P. Dineshkumar, M. Venkatesan, Review on nanofluids characterization, heat transfer characteristics and applications, Renew. Sustain. Energy Rev. 64 (2016) 163–173.
[6] M.U. Sajid, H.M. Ali, Recent advances in application of nanofluids in heat transfer devices: a critical review, Renew. Sustain. Energy Rev. 103 (2019) 556–592.
[7] S. Chakraborty, P.K. Panigrahi, Stability of nanofluid: a review, Appl. Therm. Eng. 174 (2020).
[8] A.I. Khan, A.V. Arasu, A review of influence of nanoparticle synthesis and geometrical parameters on thermophysical properties and stability of nanofluids, Therm. Sci. Eng. Prog. 11 (2019) 334–364.
[9] K.R. Aglawe, R.K. Yadav, S.B. Thool, Preparation, applications and challenges of nanofluids in electronic cooling: a systematic review, Mater. Today Proc. 43 (2021) 366–372.
[10] N. Putra, Yanuar, F.N. Iskandar, Application of nanofluids to a heat pipe liquid-block and the thermoelectric cooling of electronic equipment, Exp. Therm. Fluid Sci. 35 (2011) 1274–1281.
[11] S.S. Meibodi, A. Kianifar, O. Mahian, S. Wongwises, Second law analysis of a nanofluid-based solar collector using experimental data, J. Therm. Anal. Calorim. 126 (2016) 617–625.
[12] G.T. Hu, X. Ning, M. Hussain, U. Sajjad, M. Sultan, H.M. Ali, T.R. Shah, H. Ahmad, Potential evaluation of hybrid nanofluids for solar thermal energy harvesting: a review of recent advances, Sustain Energy Techn 48 (2021).
[13] V. Bhalla, H. Tyagi, Solar energy harvesting by cobalt oxide nanoparticles, a nanofluid absorption based system, Sustain Energy Techn 24 (2017) 45–54.
[14] S.M. Aminossadati, B. Ghasemi, Natural convection cooling of a localised heat source at the bottom of a nanofluid-filled enclosure, Eur. J. Mech. B Fluid 28 (2009) 630–640.
[15] S.P. Jang, S.U.S. Choi, Cooling performance of a microchannel heat sink with nanofluids, Appl. Therm. Eng. 26 (2006) 2457–2463.
[16] K.Y. Leong, R. Saidur, S.N. Kazi, A.H. Mamun, Performance investigation of an automotive car radiator operated with nanofluid-based coolants (nanofluid as a coolant in a radiator), Appl. Therm. Eng. 30 (2010) 2685–2692.
[17] S. Masood, M. Farooq, S. Ahmad, Description of viscous dissipation in magnetohydrodynamic flow of nanofluid: applications of biomedical treatment, Adv. Mech. Eng. 12 (2020).
[18] M. Sheikhpour, M. Arabi, A. Kasaeian, A.R. Rabei, Z. Taherian, Role of nanofluids in drug delivery and biomedical technology: methods and applications, Nanotechnol. Sci. Appl. 13 (2020) 47–59.
[19] S.S. Rahman, M.Z.I. Ashraf, A.K.M.N. Amin, M.S. Bashar, M.F.K. Ashik, M. Kamruzzaman, Tuning nanofluids for improved lubrication performance in turning biomedical grade titanium alloy, J. Clean. Prod. 206 (2019) 180–196.
[20] E. Bellos, Z. Said, C. Tzivanidis, The use of nanofluids in solar concentrating technologies: a comprehensive review, J. Clean. Prod. 196 (2018) 84–99.
[21] W.J. Chen, C.J. Zou, X.K. Li, Application of large-scale prepared MWCNTs nanofluids in solar energy system as volumetric solar absorber, Sol. Energy Mater. Sol. Cell. (2019) 200.
[22] F.Q. Wang, Z.M. Cheng, J.Y. Tan, Y. Yuan, Y. Shuai, L.H. Liu, Progress in concentrated solar power technology with parabolic trough collector system: a comprehensive review, Renew. Sustain. Energy Rev. 79 (2017) 1314–1328.
[23] A.B. Awan, M.N. Khan, M. Zubair, E. Bellos, Commercial parabolic trough CSP plants: research trends and technological advancements, Sol. Energy 211 (2020) 1422–1458.
[24] M.T. Islam, N. Huda, A.B. Abdullah, R. Saidur, A comprehensive review of state-of-the-art concentrating solar power (CSP) technologies: current status and research trends, Renew. Sustain. Energy Rev. 91 (2018) 987–1018.
[25] J.A. Mathews, M.C. Hu, C.Y. Wu, Concentrating solar power: a renewable energy frontier, Carbon Manag. 5 (2014) 293–308.
[26] R. Pitz-Paal, A. Amin, M.O. Bettzuge, P. Eames, G. Flamant, F. Fabrizi, J. Holmes, A. Kribus, H. van der Laan, C. Lopez, F.G. Novo, P. Papagiannakopoulos, E. Pihl, P. Smith, H.J. Wagner, Concentrating solar power in europe, the Middle East and North africa: a review of development issues and potential to 2050, J Sol Energ-T Asme 134 (2012).
[27] G.E. Arnaoutakis, D.A. Katsaprakakis, Concentrating solar power advances in geometric Optics, materials and system integration, Energies 14 (2021).
[28] Q.J. Mao, Recent developments in geometrical configurations of thermal energy storage for concentrating solar power plant, Renew. Sustain. Energy Rev. 59 (2016) 320–327.

[29] M. Liu, N.H.S. Tay, S. Bell, M. Belusko, R. Jacob, G. Will, W. Saman, F. Bruno, Review on concentrating solar power plants and new developments in high temperature thermal energy storage technologies, Renew. Sustain. Energy Rev. 53 (2016) 1411–1432.
[30] A. Khalil, M. Amjad, F. Noor, A. Hussain, S. Nawaz, E.P. Bandarra, X.Z. Du, Performance analysis of direct absorption-based parabolic trough solar collector using hybrid nanofluids, J. Braz. Soc. Mech. Sci. 42 (2020).
[31] D.D. Zidan, C.B. Maia, M.R. Safaei, Performance evaluation of various nanofluids for parabolic trough collectors, Sustain Energy Techn 50 (2022).
[32] K. Vignarooban, X.H. Xu, A. Arvay, K. Hsu, A.M. Kannan, Heat transfer fluids for concentrating solar power systems - a review, Appl. Energy 146 (2015) 383–396.
[33] F. Rubbi, L. Das, K. Habib, N. Aslfattahi, R. Saidur, M.T. Rahman, State-of-the-art review on water-based nanofluids for low temperature solar thermal collector application, Sol. Energy Mater. Sol. Cell. 230 (2021), 111220.
[34] Q. Gao, Y. Lu, Q. Yu, Y. Wu, C. Zhang, R. Zhi, High-temperature corrosion behavior of austenitic stainless steel in quaternary nitrate molten salt nanofluids for concentrated solar power, Sol. Energy Mater. Sol. Cell. 245 (2022), 111851.
[35] N. Navarrete, U. Nithiyanantham, L. Hernández, R. Mondragón, K2CO3–Li2CO3 molten carbonate mixtures and their nanofluids for thermal energy storage: an overview of the literature, Sol. Energy Mater. Sol. Cell. 236 (2022), 111525.
[36] G. Puliti, S. Paolucci, M. Sen, Nanofluids and their properties, Appl. Mech. Rev. 64 (2011).
[37] T. Hu, J. Zhang, J. Whyte, B. Fu, C. Song, W. Shang, P. Tao, T. Deng, Silicone oil nanofluids dispersed with mesoporous crumpled graphene for medium-temperature direct absorption solar-thermal energy harvesting, Sol. Energy Mater. Sol. Cell. 243 (2022), 111794.
[38] Z. Said, M. Ghodbane, B. Boumeddane, A.K. Tiwari, L.S. Sundar, C. Li, N. Aslfattahi, E. Bellos, Energy, exergy, economic and environmental (4E) analysis of a parabolic trough solar collector using MXene based silicone oil nanofluids, Sol. Energy Mater. Sol. Cell. 239 (2022), 111633.
[39] H. Olia, M. Torabi, M. Bahiraei, M.H. Ahmadi, M. Goodarzi, M.R. Safaei, Application of nanofluids in thermal performance enhancement of parabolic trough solar collector: state-of-the-art, Appl Sci-Basel 9 (2019).
[40] R. Naveenkumar, P.C. Santhosh Kumar, M. Dinesh Kumar, M. Ravichandran, Review on nanofluid role & design aspects to enhance the thermal performance of the parabolic trough collector, AIP Conf. Proc. 2283 (2020), 020135.
[41] M. Milanese, G. Colangelo, A. Cretì, M. Lomascolo, F. Iacobazzi, A.d. Risi, Optical absorption measurements of oxide nanoparticles for application as nanofluid in direct absorption solar power systems – Part II: ZnO, CeO2, Fe2O3 nanoparticles behavior, Sol. Energy Mater. Sol. Cell. 147 (2016) 321–326.
[42] I. Carrillo-Berdugo, P. Estellé, E. Sani, L. Mercatelli, R. Grau-Crespo, D. Zorrilla, J. Navas, Optical and transport properties of Metal−Oil nanofluids for thermal solar industry: experimental characterization, performance assessment, and molecular dynamics insights, ACS Sustain. Chem. Eng. 9 (2021) 4194–4205.
[43] E. Torres, I. Carrillo-Berdugo, D. Zorrilla, J. Sánchez-Márquez, J. Navas, CuO-containing oil-based nanofluids for concentrating solar power: an experimental and computational integrated insight, J. Mol. Liq. 325 (2021), 114643.
[44] R. Lv, J.A. Robinson, R.E. Schaak, D. Sun, Y.F. Sun, T.E. Mallouk, M. Terrones, Transition metal dichalcogenides and beyond: synthesis, properties, and applications of single- and few-layer nanosheets, Accounts Chem. Res. 48 (2015) 56–64.
[45] T. Chowdhury, E.C. Sadler, T.J. Kempa, Progress and prospects in transition-metal dichalcogenide research beyond 2D, Chem. Rev. 120 (2020) 12563–12591.
[46] S. Manzeli, D. Ovchinnikov, D. Pasquier, O.V. Yazyev, A. Kis, 2D transition metal dichalcogenides, Nat. Rev. Mater. 2 (2017).
[47] V. Nicolosi, M. Chhowalla, M.G. Kanatzidis, M.S. Strano, J.N. Coleman, Liquid exfoliation of layered materials, Science 340 (2013) 1420(. -+).
[48] Y. Hernandez, V. Nicolosi, M. Lotya, F.M. Blighe, Z.Y. Sun, S. De, I.T. McGovern, B. Holland, M. Byrne, Y.K. Gun'ko, J.J. Boland, P. Niraj, G. Duesberg, S. Krishnamurthy, R. Goodhue, J. Hutchison, V. Scardaci, A.C. Ferrari, J. N. Coleman, High-yield production of graphene by liquid-phase exfoliation of graphite, Nat. Nanotechnol. 3 (2008) 563–568.
[49] J.F. Shen, Y.M. He, J.J. Wu, C.T. Gao, K. Keyshar, X. Zhang, Y.C. Yang, M.X. Ye, R. Vajtai, J. Lou, P.M. Ajayan, Liquid phase exfoliation of two-dimensional materials by directly probing and matching surface tension components, Nano Lett. 15 (2015) 5449–5454.
[50] J. Navas, P. Martinez-Merino, A. Sanchez-Coronilla, J.J. Gallardo, R. Alcantara, E. I. Martin, J.C. Pinero, J.R. Leon, T. Aguilar, J.H. Toledo, C. Fernandez-Lorenzo, MoS2 nanosheets vs. nanowires: preparation and a theoretical study of highly stable and efficient nanofluids for concentrating solar power, J. Mater. Chem. 6 (2018) 14919–14929.
[51] M. Teruel, T. Aguilar, P. Martinez-Merino, I. Carrillo-Berdugo, J.J. Gallardo-Bernal, R. Gomez-Villarejo, R. Alcantara, C. Fernandez-Lorenzo, J. Navas, 2D MoSe2-based nanofluids prepared by liquid phase exfoliation for heat transfer applications in concentrating solar power, Sol. Energy Mater. Sol. Cell. (2019) 200.
[52] S.U. Ilyas, R. Pendyala, N. Marneni, Preparation, sedimentation, and agglomeration of nanofluids, Chem. Eng. Technol. 37 (2014) 2011–2021.
[53] P.D. Shima, J. Philip, B. Raj, Influence of aggregation on thermal conductivity in stable and unstable nanofluids, Appl. Phys. Lett. 97 (2010).
[54] T. Aguilar, J. Navas, A. Sanchez-Coronilla, E.I. Martin, J.J. Gallardo, P. Martinez-Merino, R. Gomez-Villarejo, J.C. Pinero, R. Alcantara, C. Fernandez-Lorenzo, Investigation of enhanced thermal properties in NiO-based nanofluids for concentrating solar power applications: a molecular dynamics and experimental analysis, Appl. Energy 211 (2018) 677–688.
[55] J.N. Coleman, M. Lotya, A. O'Neill, S.D. Bergin, P.J. King, U. Khan, K. Young, A. Gaucher, S. De, R.J. Smith, I.V. Shvets, S.K. Arora, G. Stanton, H.Y. Kim, K. Lee, G.T. Kim, G.S. Duesberg, T. Hallam, J.J. Boland, J.J. Wang, J.F. Donegan, J. C. Grunlan, G. Moriarty, A. Shmeliov, R.J. Nicholls, J.M. Perkins, E.M. Grieveson, K. Theuwissen, D.W. McComb, P.D. Nellist, V. Nicolosi, Two-dimensional nanosheets produced by liquid exfoliation of layered materials, Science 331 (2011) 568–571.
[56] M.I. Pryazhnikov, A.V. Minakov, V.Y. Rudyak, D.V. Guzei, Thermal conductivity measurements of nanofluids, Int. J. Heat Mass Tran. 104 (2017) 1275–1282.
[57] E.V. Timofeeva, W.H. Yu, D.M. France, D. Singh, J.L. Routbort, Nanofluids for heat transfer: an engineering approach, Nanoscale Res. Lett. 6 (2011).
[58] M. Eagleson, Concise Encyclopedia Chemistry, 1994.
[59] S.M.S. Murshed, P. Estelle, A state of the art review on viscosity of nanofluids, Renew. Sustain. Energy Rev. 76 (2017) 1134–1152.
[60] M. Awais, N. Ullah, J. Ahmad, F. Sikandar, M.M. Ehsan, S. Salehin, A.A. Bhuiyan, Heat transfer and pressure drop performance of Nanofluid: a state-of- the-art review, International Journal of Thermofluids 9 (2021), 100065.
[61] S.M.S. Murshed, Determination of effective specific heat of nanofluids, J. Exp. Nanosci. 6 (2011) 539–546.
[62] I.M. Shahrul, I.M. Mahbubul, S.S. Khaleduzzaman, R. Saidur, M.F.M. Sabri, A comparative review on the specific heat of nanofluids for energy perspective, Renew. Sustain. Energy Rev. 38 (2014) 88–98.
[63] R. Gómez-Villarejo, E.I. Martín, A. Sánchez-Coronilla, T. Aguilar, J.J. Gallardo, P. Martínez-Merino, I. Carrillo-Berdugo, R. Alcántara, C. Fernández-Lorenzo, J. Navas, Towards the improvement of the global efficiency of concentrating solar power plants by using Pt-based nanofluids: the internal molecular structure effect, Appl. Energy 228 (2018) 2262–2274.
[64] P. Martínez-Merino, A. Sánchez-Coronilla, R. Alcántara, E.I. Martín, J. Navas, Insights into the stability and thermal properties of WSe2 -based nanofluids for concentrating solar power prepared by liquid phase exfoliation, J. Mol. Liq. 319 (2020), 114333.
[65] R. Hentschke, On the specific heat capacity enhancement in nanofluids, Nanoscale Res. Lett. 11 (2016) 88.
[66] D. Shin, D. Banerjee, Enhancement of specific heat capacity of high-temperature silica-nanofluids synthesized in alkali chloride salt eutectics for solar thermal-energy storage applications, Int. J. Heat Mass Tran. 54 (2011) 1064–1070.
[67] L. Xue, P. Keblinski, S.R. Phillpot, S.U.S. Choi, J.A. Eastman, Effect of liquid layering at the liquid–solid interface on thermal transport, Int. J. Heat Mass Tran. 47 (2004) 4277–4284.
[68] R. Prasher, P. Bhattacharya, P.E. Phelan, Thermal conductivity of nanoscale colloidal solutions (nanofluids), Phys. Rev. Lett. 94 (2005), 025901.
[69] J.J. Wang, R.T. Zheng, J.W. Gao, G. Chen, Heat conduction mechanisms in nanofluids and suspensions, Nano Today 7 (2012) 124–136.
[70] J. Buongiorno, Convective transport in nanofluids, J. Heat Tran. 128 (2005) 240–250.
[71] Y. Xuan, Q. Li, W. Hu, Aggregation structure and thermal conductivity of nanofluids, AIChE J. 49 (2003) 1038–1043.
[72] A. Nasiri, M. Shariaty-Niasar, A.M. Rashidi, R. Khodafarin, Effect of CNT structures on thermal conductivity and stability of nanofluid, Int. J. Heat Mass Tran. 55 (2012) 1529–1535.
[73] J. Glory, M. Bonetti, M. Helezen, M. Mayne-L'Hermite, C. Reynaud, Thermal and electrical conductivities of water-based nanofluids prepared with long multiwalled carbon nanotubes, J. Appl. Phys. 103 (2008), 094309.
[74] M. Farbod, R. Kouhpeymani asl, A.R. Noghreh abadi, Morphology dependence of thermal and rheological properties of oil-based nanofluids of CuO nanostructures, Colloids Surf. A Physicochem. Eng. Asp. 474 (2015) 71–75.
[75] H. Xie, J. Wang, T. Xi, Y. Liu, Thermal conductivity of suspensions containing nanosized SiC particles, Int. J. Thermophys. 23 (2002) 571–580.
[76] S. Kakaç, A. Pramuanjaroenkij, Review of convective heat transfer enhancement with nanofluids, Int. J. Heat Mass Tran. 52 (2009) 3187–3196.
[77] E. Bellos, C. Tzivanidis, Analytical expression of parabolic trough solar collector performance, Design 2 (2018) 9.
[78] G.J. O'Keeffe, S.L. Mitchell, T.G. Myers, V. Cregan, Modelling the efficiency of a nanofluid-based direct absorption parabolic trough solar collector, Sol. Energy 159 (2018) 44–54.
[79] T.L. Bergman, A.S. Lavine, F.P. Incropera, D.P. Dewitt, Fundamentals of Heat and Mass Transfer, seventh ed., John Wiley & Sons, New Jersey, USA, 2011.